Supplementary Materials

Flow Simulations

Due to the expansion of the channel around the electrodes there is a chance of turbulent flow in the cavities at the electrodes. However, due the sloped channel walls of the expansion, rounded corners of the expanded area (see Figure S1), as well as the low flow rate, and a Reynolds number way below 1 for both the channel and area around the electrodes (see Table S1). The chance of any turbulent flow in the expanded areas is limited.

Table S1. Reynolds numbers for the different parts of the optimized system and the values used for the calculation.

Part	Channel height	Channel width	Flow rate	Flow velocity	Reynolds number
Channel	5.00×10^{-6}	1.00×10^{-5}	2.00×10^{-8}	6.60×10^{-3}	0.04
Electrodes	5.00×10^{-6}	2.00×10^{-5}	2.00×10^{-8}	3.30×10^{-3}	2.40×10^{-2}

Finite element modeling (FEM) of the flow through the channel was simulated using COMSOL 4.3a (COMSOL AB, Kgs. Lyngby, Denmark). The simulations of the flow in the expanded of the channel around the electrodes where done using the laminar flow module with no-slip boundary conditions. The medium was defined as water using the built-in material parameters of COMSOL. The inlet flow of the channel was set to 1×10^{-9} kg/s (60 nL/min).

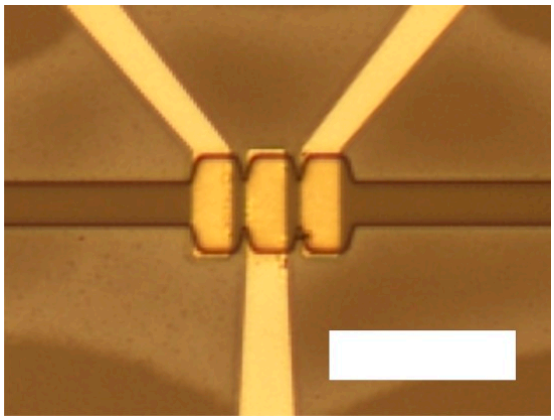

Figure S1. Optical image of the electrode layout of the optimized design. The white bar is 50 μm.

Figure S2A shows the simulated the *x*-component of the flow velocity, while Figure S2B shows the *y*-component of the flow velocity for the optimized system. As can be seen from the simulations of the flow velocities, ones observes that the *x*-component decreases in the cavities at the electrodes (and hence changes the shape of the measured signal see Figure 5), while the y-component goes into the cavities at the entrance, which would force any particles in the liquid into the cavities and goes back in to the channel at the exit. This could in principle be a source for particle trapping in the cavity, however, the authors did not notice any particles left in the cavities after experiments. Table S2 contains the signal to noise ratio of the measured signal in Figure 5.

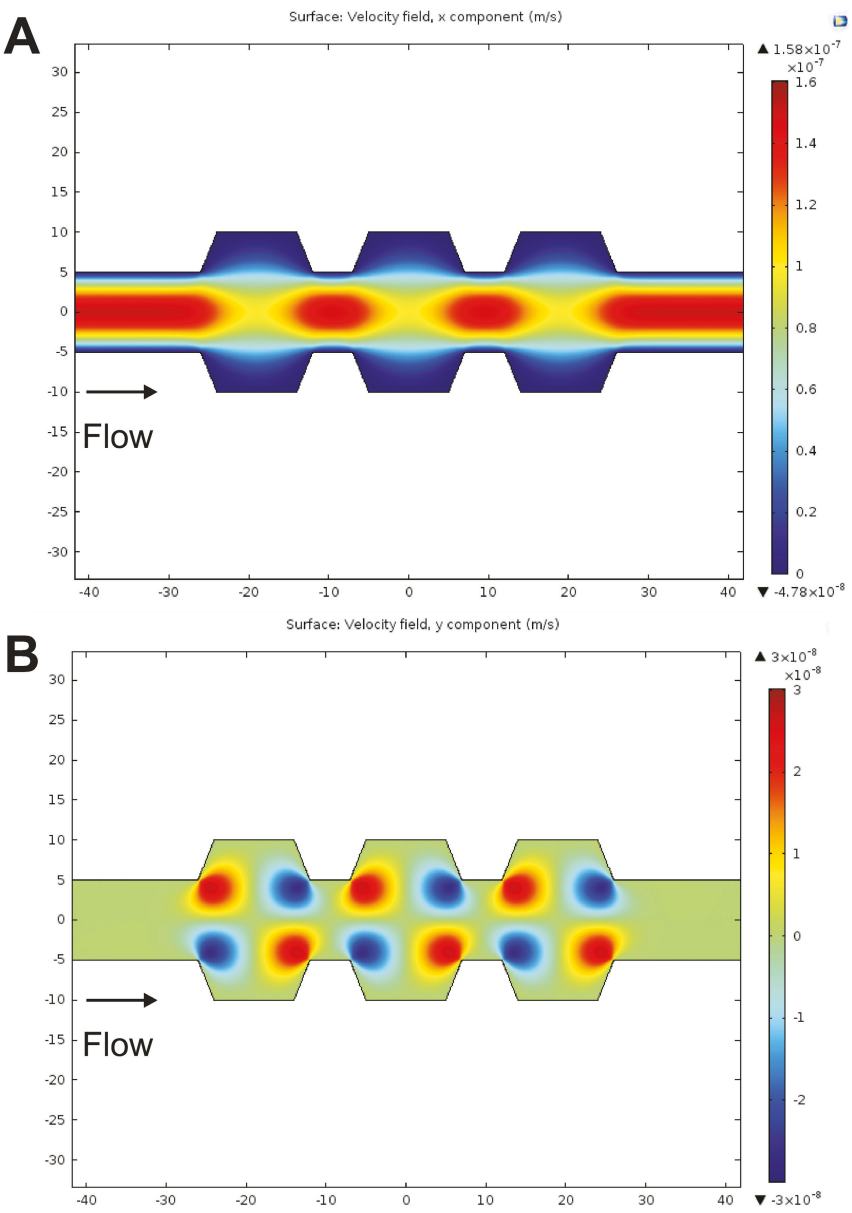

Figure S2. COMSOL simulations of the flow velocity in the optimized chip layout. (**A**) The *x*-component of the flow velocity. (**B**) The *y*-component of the flow velocity.

Table S2. Signal to noise ratio for the different tansitions shown in Figure 5.

Optimized 2 µm re	Optimized 2 µm im	Optimized 1 µm re	Optimized 1 µm im	Optimized 0.5 µm re	Optimized 05 µm im	Conventional 2 µm re	Conventional 2 µm im	Conventional 1 µm re	Conventional 1 µm im
2.79×10^2	1.11×10^2	4.31×10^1	1.78×10^1	1.33×10^1	4.93	2.02×10^2	1.54×10^2	3.54×10^1	2.72×10^1